

Defect charge states in Si doped hexagonal boron-nitride monolayer

R. E. Mapasha,^{1,*} M. P. Molepo,¹ R. C. Andrew,¹ and N. Chetty^{1,2}

¹*Department of Physics, University of Pretoria, Pretoria 0002, South Africa*

²*National Institute for Theoretical Physics, Johannesburg, 2000, South Africa*

(Dated: December 14, 2015)

Abstract

We perform *ab-initio* density functional theory calculations to investigate the energetics, electronic and magnetic properties of isolated stoichiometric and non-stoichiometric substitutional Si complexes in a hexagonal boron-nitride monolayer. The Si impurity atoms substituting the boron atom sites Si_B giving non-stoichiometric complexes are found to be the most energetically favourable, and are half-metallic and order ferromagnetically in the neutral charge state. We find that the magnetic moments and magnetization energies increase monotonically when Si defects form a cluster. Partial density of states and standard Mulliken population analysis indicate that the half-metallic character and magnetic moments mainly arise from the Si $3p$ impurity states. The stoichiometric Si complexes are energetically unfavorable and non-magnetic. When charging the energetically favourable non-stoichiometric Si complexes, we find that the formation energies strongly depend on the impurity charge states and Fermi level position. We also find that the magnetic moments and orderings are tunable by charge state modulation $q = -2, -1, 0, +1, +2$. The induced half-metallic character is lost (retained) when charging isolated (clustered) Si defect(s). This underlines the potential of a Si doped hexagonal boron-nitride monolayer for novel spin-based applications.

INTRODUCTION

After its experimental synthesis in 2004 [1], single layer hexagonal boron nitride (*h*-BN) continues to gain research attention because of its peculiar physical and chemical properties [2–5] similar to graphene [6–10]. The measured extreme hardness, high melting point, high thermal conductivity and large exciton binding energies [1, 11, 12] make *h*-BN monolayer a possible material for potential use in high-performance solid state electronic devices. Despite its isostructural arrangement, *h*-BN monolayer is an insulator with a band gap of about 5 eV [1, 11, 12] whereas graphene is semi-metallic in nature [8].

Recent characterizations of non-metal doped *h*-BN monolayer revealed interesting features such as magnetism and half-metallic character. [13–21] These special features make the non-metal doped *h*-BN system a potential candidate for spin-based device exploitation (which utilizes the electronic spin states for data storage and processing). The search for suitable Half-Metallic-Ferromagnet (HMFM) materials started in 1983 after the De Groot *et al.* [22] discovery. Most of the promising HMFM systems are those made by doping magnetic transition metals in group III-VI and II-V semiconductors. [23–25] However, the relatively low Curie temperature [25], that can be below the room temperature for these systems, is a limiting feature for their applications in spin-based electronic devices. Layered systems as peculiar materials have an estimated Curie temperature far higher than room temperature. [21] Moreover, the realization of the induced magnetism in these non-magnetic materials when exposed to non-metals ignited huge research attention. [13–21] A lot of interest is on the understanding of the origin of magnetism, and its impact on the known physical properties of layered systems.

The energetics, electronic and magnetic properties of boron or nitrogen vacancy (v_B or v_N), boron (B), nitrogen (N) and carbon (C) defects in *h*-BN monolayer were extensively studied. [15, 16, 20, 26–34] Si *et al.* [16] reported that v_B is more energetically preferable than v_N vacancy. They also found that both vacancies induce spontaneous magnetization, with v_B possessing half-metallic character. Other study by Huang *et al.* [35], examined the effects of various charge states on the vacancies in *h*-BN monolayer. It was found that the structural properties around the vacancy defect are sensitive to charge states due to the effects of dangling bonds. Carbon atoms are some of the unintentional defects that spontaneously occur during the growth of a *h*-BN monolayer. [5, 36, 37] There is no observed significant structural distortion in the C doped *h*-BN monolayer due to small lattice mismatch of about 2%. [5] The intentional creation of C doped *h*-BN monolayer using *in*

situ electron-beam irradiation revealed that only the B sites are occupied. [19] The carbon impurity atoms do not only alter the known electronic properties of the pristine host but also provide a new interesting character. [19, 38–41] It was reported that the C impurity spontaneously induces magnetization and half-metallic character. [19–21, 38–41] Ukpong *et al.* [21] have shown via DFT calculations that the induced magnetic moments are easily affected by the size of the embedded C impurity cluster and edge termination. Berseneva *et al.* [20] reported that the C substitution processes are controlled by the energetics of the atomic configurations, more especially when the system is charged. They also reported that charge variation is able to switch on and off the induced magnetism of the C clusters.

Silicon (Si) which belongs to the carbon group has recently been incorporated in *h*-BN monolayer. [15, 42–47] Using DFT methods, Liu *et al.* [47] revealed that the Si impurity prefers the B site, but as opposed to C, it severely deforms the *h*-BN structure preserving the sp^3 -like bonding. It can also enhance the chemical reactivity of *h*-BN monolayer. He *et al.* [43] showed, via Hall effect and temperature-dependent resistivity measurements, n-type conduction with a low resistivity at room temperature and two shallow donor levels at high temperature of about 800 K when the Si occupies the B site. On the other hand, Majety *et al.* [45] reported a deep donor level of about 1.20 eV using the same technique and concluded that Si-doped *h*-BN is not suitable for room temperature device applications. Inspired by the experimental realization of Si-doped *h*-BN monolayers, [44, 45] a systematic study of the physical properties of various possible Si atomic configurations will be interesting. Also, the knowledge of the dependence of physical properties for a Si-doped *h*-BN monolayer on the defect charge states is still scarce.

In this paper, we report the energetics, electronic and magnetic behavior of the various charged substitutional Si impurity complexes in *h*-BN layer. In this study, the Si impurity complexes are created as follows; firstly, one B as a host atom is removed from the *h*-BN monolayer and is replaced by a Si atom (Si impurity occupying B site Si_B). Secondly, one N atom as a host atom is removed from the monolayer and is replaced by a Si atom (Si impurity occupying N site Si_N). Furthermore, several unique complexes consisting of two or three substitutional Si impurities are explored. The origin of Si impurity induced half-metallic character is investigated based on partial density of states and standard Mulliken population analysis. We established that the Si impurity induced ordered magnetic moments are tunable by impurity charge states modulation.

COMPUTATIONAL DETAILS

All the ground state properties of Si impurity substitutional complexes in *h*-BN are calculated using the DFT method implemented within the Vienna *ab-initio* simulation package (VASP). [48–51] In order to treat the exchange-correlation energy interactions, the generalized gradient approximation based on Perdew-Burke-Ernzerhof parametrization (GGA-PBE)[52] was employed. The projector augmented wave (PAW) method [53] was used in the generation of pseudopotentials that take care of valence-core electronic interactions.

We used a kinetic energy cutoff of 500 eV for the expansion of one-electron Kohn-Sham wave functions on the plane-wave basis. A $4 \times 4 \times 1$ mesh of *k*-points generated using Monkhorst Pack scheme [54] was used for sampling the Brillouin zone. All the atomic geometries were allowed to relax freely based on the Hellman-Feymann theorem until the maximum allowed force on each atom is less than 0.002 eV/Å. The total energy was allowed to converge to within 10^{-7} eV. The electronic states were populated using the Methfessel-Paxton scheme [55] in the self-consistent field calculations, with a smearing width of 0.3 eV. A converged vacuum spacing of 15 Å between two adjacent *h*-BN monolayers is used for the prevention of spurious interlayer interaction within the periodic supercell simulation scheme. Since we were interested in an isolated layer, van der Waals correlations were not included.

RESULTS AND DISCUSSION

Formation energies of Si substitutional complexes

Figure 1(a) shows the ball and stick models for different unrelaxed Si substitutional complexes considered in this study. In *h*-BN monolayer, each hexagon ring consists of three B atoms located at the odd sites and three N atoms at the even sites as indicated on Fig 1(a). Each circle on Fig 1(a) depicts a unique stoichiometric or non-stoichiometric complex examined on a 72 atom supercell of *h*-BN.

The non-stoichiometric Si_{B1} complex is obtained when a single Si impurity atom substitutes the B atom at site 1, whereas the Si_{N2} complex is obtained when Si atom substitutes the nitrogen at atomic site 2. Taking the possibility of two Si impurity atoms into account, four unique Si complexes are identified and presented in Fig. 1(a). The stoichiometric complex Si_{B1N2} is obtained

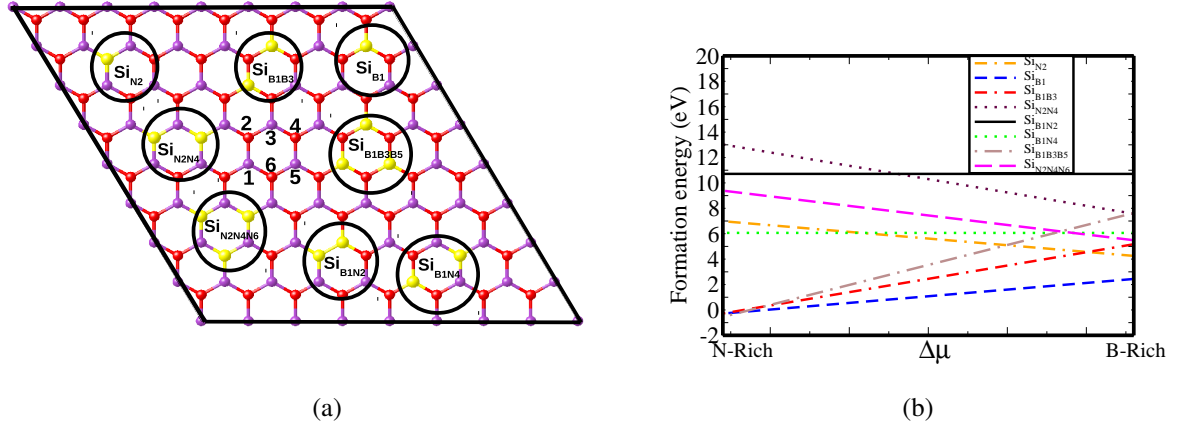


FIG. 1. (Colour online) (a) Identified Si substitutional impurity defect complexes in *h*-BN monolayer. The purple, red and yellow spheres represent boron, nitrogen and silicon atoms respectively. In *h*-BN above, each hexagon ring consists of three B atoms located on the odd sites and three N atoms always on the even sites. (b) The calculated formation energies of all Si impurity complexes presented in Fig. 1(a) in the neutral state.

when two Si impurity atoms each substitutes B and N at nearest neighbour lattice sites 1 and 2 respectively, whereas Si_{B1N4} is found when Si atom is at site 1 and site 4 (i.e substituting B and N respectively). Similarly, the non-stoichiometric complexes are obtained when two B atoms at lattice sites 1 and 3 (Si_{B1B3}) or two N atoms at lattice sites 2 and 4 (Si_{N2N4}) are substituted by Si impurity atoms. On the other hand, when three Si impurity atoms substitute three B or N atoms, the non-stoichiometric complexes $\text{Si}_{\text{B1B3B5}}$ or $\text{Si}_{\text{N2N4N6}}$ are studied.

Supercell sizes of 3×3 , 4×4 , 5×5 , 6×6 and 7×7 corresponding to 18, 32, 50, 72 and 98 atoms are employed for convergence test considering Si_{B1} and Si_{N2} complexes. The total energy difference ΔE between the pristine and defected *h*-BN system was calculated for each supercell size. For the Si_{B1} complex, ΔE is -4.72 eV, -4.38 eV, -4.27 eV, -4.23 eV and -4.28 eV, while for the Si_{N2} ΔE is -10.80 eV, -10.55 eV, -10.38 eV, -10.36 eV and -10.34 eV for different supercell sizes 3×3 , 4×4 , 5×5 , 6×6 and 7×7 . For both complexes, the change in ΔE shows convergence for the 5×5 supercell. Since this study involves the incorporation of 1-3 Si impurity atoms, the 6×6 supercell is employed in all of our calculations.

Firstly, we use the nudged elastic band method [56–58] implemented in VASP to evaluate the

energy barrier for Si impurity atom either occupying the B site (Si_{B1}) or occupying the N site (Si_{N2}). For initial configuration of (Si_{B1}), we create the B vacancy and place the Si impurity 3 Å above the vacancy as the start of the doping process. For the final configuration, the coordinates of the relaxed Si_{B1} configuration presented in figure 4 are used. The same approach was followed for the calculation of Si_{N2} barrier. The energy barrier was obtained by optimizing five images between the initial configuration and the final configuration along the reaction coordinate. We carried out the full structure optimization for the transition states and only searched for the highest saddle point. For Si_{B1} and Si_{N2} defects, we obtained the energy barriers of 0.34 eV and 1.09 eV respectively. Majety *et al.* [45] experimentally reported the two activation energies of 15 meV in 50-300 K and 60 meV in 300-800 K for Si_B in the *h*-BN monolayer. Yin *et al.* [59] reported the activation energy of 0.4 eV for Si_B in the cubic BN monolayer at the temperature of 470 K. The relatively high energy barrier for Si_{N2} defect is not surprising because previous study reported that Si impurity prefers occupying the B site as compared to the N site. [47] The formation energies of these defects are discussed in the next paragraph.

To examine the formation possibility of the above-mentioned Si impurity substitutional complexes in the neutral charge state ($q = 0$), their formation energies are calculated using the following equation;

$$E_f[\text{Si}]^0 = E_{tot}[\text{Si} : h\text{-BN}]^0 - E_{tot}[h\text{-BN}] + n_i\mu_i - n_{\text{Si}}\mu_{\text{Si}}, \quad (1)$$

where $E_{tot}[\text{Si} : h\text{-BN}]^0$ and $E_{tot}[h\text{-BN}]$ terms are the total energies of the relaxed *h*-BN supercell with and without Si atoms (pristine), respectively. n_i indicates the total number of B or N replaced, and n_{Si} is the number of Si impurities in the *h*-BN supercell. μ_i and μ_{Si} are the corresponding atomic chemical potentials for B or N and Si respectively. The N and B chemical potentials are taken from nitrogen gas (N_2) and α -rhombohedral boron, respectively and Si is from the diamond structure. The chemical potential represents the Gibbs free energy which isolated atoms exchange with the heat reservoir.

The dependence of formation energies of the considered Si impurity complexes on the changes in the atomic chemical potentials ($\Delta\mu$) are examined in Fig 1(b). The enthalpy of formation $\Delta H_f[h\text{-BN}]$ of the pristine *h*-BN monolayer calculated using $\Delta H_f[h\text{-BN}] = \mu_{h\text{-BN}} - \mu_B - \mu_N$ is -2.64 eV (-2.58 eV [60], -2.60 ± 0.02 eV[61]). The calculation is based on the thermodynamic equilibrium condition that $\mu_{h\text{-BN}} = \mu_B + \mu_N$, such that the chemical potentials μ_B and μ_N can be subjected to the upper bounds under extreme condition. [62] The obtained value is used to restrict

the $\Delta\mu$, i.e. $-2.64 \text{ eV} \leq \Delta\mu \leq 2.64 \text{ eV}$ so that the variation in calculated formation energy should be confined within this interval. These energy limits -2.64 eV and 2.64 eV are considered to be N-rich and B-rich conditions respectively. This will indicate the growth condition in which these systems will prefer to form.

Fig 1(b) shows that the non-stoichiometric Si_{B1} (-0.29 eV), Si_{B1B3} (-0.29 eV) and Si_{B1B3B5} (-0.54 eV) complexes prefer to form in the N-rich condition, whereas the Si_{N2} (4.19 eV), Si_{N2N4} (5.45 eV) and Si_{N2N4N6} (7.42 eV) complexes prefer the B-rich condition in the neutral charge state. This implies that an enhanced Si defect stability is obtained in the environment that corresponds to the high amount of atomic species surrounding the defect in the *h*-BN. Berseneva *et al.* [20] reported that the substitution of B with C impurity costs less energy than the substitution of N atom under N-rich conditions. This is in agreement with Murata *et al.*[44] who deposited Si atom in cubic-BN under high pressure high temperature conditions, and using X-ray diffraction found that Si spontaneously occupies B site and get surrounded by four nitrogen atoms. We also see that the formation energies of Si_{B1} , Si_{B1B3} and Si_{B1B3B5} are approximately 0 eV in the N-rich condition, but diverges significantly when approaching the B-rich conditions. Moreover, although the Si_{B1} complex prefers the N-rich condition, we also notice that it presents the lowest formation energy of 2.36 eV in the B-rich condition in the neutral charge state shown in Fig 1(b). This implies that the Si_{B1} complex may still form under B-rich conditions. Our results also show that the formation of Si-N bond (exothermic) in *h*-BN monolayer requires less energy penalty than the formation of Si-B bond (endothermic).

Fig 1(b) also shows that the formation energies of stoichiometric complexes Si_{B1N2} and Si_{B1N4} are not sensitive to growth conditions. Ukpong *et al.* [21] observed similar behaviour in the studies of stoichiometric C complexes in *h*-BN monolayer. These stoichiometric complexes represent co-doping, because they involve the incorporation of donor (Si_B) together with acceptor (Si_N) in *h*-BN monolayer. This compensation results in increasing the formation energy of Si_B and lowering that of Si_N , leading to formation energies of these complexes remaining constant w.r.t. the change in chemical potential. Although the Si_{B1N2} and Si_{B1N4} complexes have the same Si concentration, their formation energies are unequal. The Si_{B1N4} complex is 4.63 eV lower in the formation energy than Si_{B1N2} in the neutral charge state. This implies that during the formation of Si_{B1N2} complex, high energy will be needed to first break the B-N bonds and spontaneously form Si-Si bond (sp^3 bond) in the sp^2 bonded system.

We further examine the effect of different charge states q ($-2, -1, 0, +1, +2$) on the stability of the

most energetically favourable complexes, i.e Si_{B1} , Si_{B1B3} and Si_{B1B3B5} . It must be pointed out that in the creation of Si_{B1} complex, one extra electron is added into the system and the possible charge states should be -1, 0, and +1. For the larger defect complexes such as Si_{B1B3} and Si_{B1B3B5} , the high charge states might be possible. The supercell formation energy $E_f[\text{Si}]^q$ of a Si substitutional impurity in $h\text{-BN}$ in the charge state q is calculated by extending Eq.(1) to include the information of q as follows,

$$E_f[\text{Si}]^q = E_{tot}[\text{Si} : h\text{-BN}]^q - E_{tot}[h\text{-BN}] + n_i\mu_i - n_{\text{Si}}\mu_{\text{Si}} + q(\mu_e - E_v), \quad (2)$$

where μ_e is the electronic chemical potential measured with respect to energy position of the valence band maximum E_v [63]. Our calculated formation energies are constrained to vary with respect to the position of the Fermi level (electronic potential μ_e) ranging from 0 eV to 5.10 eV (experimental band gap [1, 11, 12]). To eliminate the effect of spurious electrostatic interactions of the charged Si defect with its periodic images, supercell corrections for two (2D) dimensional systems were added to the supercell formation energies. [64, 65] We tested the corrections for various supercell sizes and the results for the +1 charge state are shown in Fig 2. They show that the corrected values for each supercell are almost the same. Based on this, we are confident in our choice of a 6×6 supercell with a 15\AA vacuum spacing for our calculations.

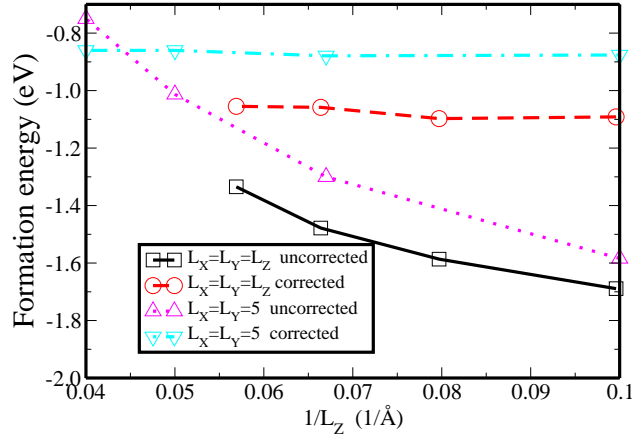


FIG. 2. (Colour online) The formation energies of Si_{B1} in the +1 charge state as a function of inverse layer separation for different supercell sizes. Two scalings were used; (1) all supercell dimensions were uniformly scaled and (2) the planar dimensions were set to 5×5 and the layer separation (L_Z) was scaled.

We further calculated the transition energy levels $\varepsilon(q/q')$ of the Si substitutional complexes using the following expression [62];

$$\varepsilon(q/q') = \frac{E_f[Si]^q - E_f[Si]^{q'}}{q' - q} \quad (3)$$

where $E_f[Si]^q$ and $E_f[Si]^{q'}$ represent formation energies of the Si substitutional complex in the charge states q and q' respectively.

The corrected formation energies of charged Si_{B1} , Si_{B1B3} and Si_{B1B3B5} as a function of the Fermi level position μ_e are presented in Fig 3, and their possible thermodynamic transition levels are summarized in Table I. Our formation energies and thermodynamic transition levels results are calculated under the N-rich growth condition. Fig 3 depicts that the formation energies of Si_{B1} , Si_{B1B3} and Si_{B1B3B5} in the neutral charge states are constant regardless of the variation in Fermi energy. Fig 3 also shows that as μ_e increases, the positively charged Si substitutional complexes show an increase in formation energy in the lower half of the band gap, while the negatively charged complexes show decrement in the upper half. This suggests that positively and negatively charged substitutional Si impurity complexes are experimentally likely to form at the valence and conduction band edges 1

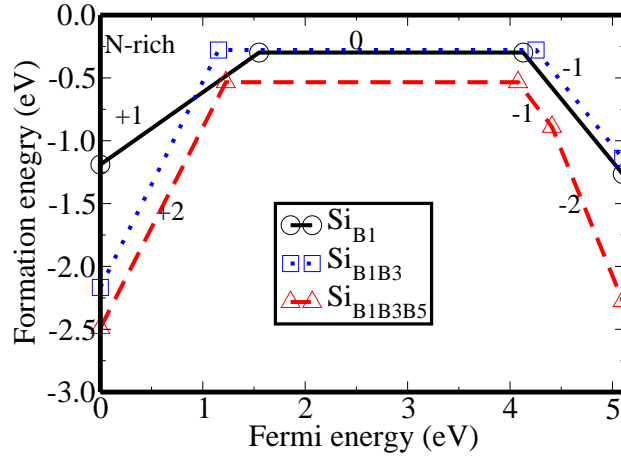


FIG. 3. (Colour online)(a) The formation energies of the most stable configurations of Si doped h -BN as a function of the Fermi level within the h -BN band gap, for different charge states (-2, -1, 0, +1 and +2). Only the line segments that correspond to the lowest energy charge states are shown. Geometric shapes in the curves indicate the transitions between the two charge states.

Fig 3 and Table I show that the introduction of negative and positive charge into the Si complexes induces respectively, acceptor or donor thermodynamic transition levels within the band

gap of h -BN. This is an indication that the charge state of a Si impurity is likely to affect properties of Si doped h -BN monolayer. The transition levels are always referenced to the band edges of pristine h -BN monolayer as follows; donor level is measured relative to the VBM (E_v) and acceptor level is referenced to CBM (E_c). In experiments, transition levels are usually determined in deep level transient spectroscopy (DLTS),[66] which forms a cornerstone for the practical identification of defects in a semiconductor.

TABLE I. Thermodynamic transition energies (in eV) of various complexes of Si doped h -BN. Energies are measured relative to the VBM (E_v) or CBM (E_c).

	(+2/0)	(+1/0)	(0/-1)	(-1/-2)
Si_{B1}	...	$E_v + 1.53$	$E_c - 0.98$...
Si_{B1B3}	$E_v + 1.15$...	$E_c - 0.86$	E_c
Si_{B1B3B5}	$E_v + 1.23$...	$E_c - 1.03$	$E_c - 0.711$

Fig 3 depicts the presence of two transition levels; (+1/0) donor and (0/-1) acceptor levels associated with the Si_{B1} complex, and these levels appear to be localized deep into the band gap at $E_v + 1.53$ eV and $E_c - 0.98$ eV respectively (see Table I). Previous studies [20, 67] have shown that the formation energies obtained using the semilocal PBE and hybrid HSE [68, 69] functionals agree very well if the electron chemical potential is re-scaled using the ratio of the band gaps obtained using the PBE and HSE approximations. The GGA-PBE functional underestimates the HSE band gap by 0.66 eV. Thus we estimate that our calculated GGA-PBE transition levels will be 0.66 eV lower than the HSE levels. For instance, the (+1/0) donor and (0/-1) acceptor levels for Si_{B1} complex obtained using HSE would be $E_v + 2.19$ eV and $E_c - 0.32$ eV respectively. Using GGA-PBE, Berseneva *et al.*[20] studied the transition levels of C_B and observed (+1/0) donor and (0/-3) acceptor levels at about $E_v + 2.70$ eV and $E_c - 0.20$ eV respectively. Although our DFT transition level values might not agree well with the experimental values owing to its weaknesses in predicting the band gaps, [70] we suggest that there might be two observable peaks due to (+1/0) and (0/-1) associated with Si_{B1} on the DLTS spectrum. Also, our results imply that the DLTS peaks associated with Si_{B1} will be observed at a higher temperature. Majety *et al.* [45] reported a deep donor level of about 1.20 eV from the temperature dependent resistivity results and also found that Si does cause n-type conduction in h -BN at relatively high temperature. They concluded that this

kind of a system is not appropriate for room temperature devices applications.

In the case of Si_{B1B3} and Si_{B1B3B5} , a donor (+1/0) transition level is not observed. Instead, the double donor (+2/0) transition level is observed at $E_v + 1.15$ eV and $E_v + 2.23$ eV for Si_{B1B3} and Si_{B1B3B5} respectively. The double acceptor (-1/-2) transition energy level associated with Si_{B1B3} lies exactly at the CBM, which will not be practical for DLTS to identify this particular level. The double acceptor (-1/-2) level associated with Si_{B1B3B5} appear to be localized deep at $E_c - 0.711$ eV. This suggests that non-stoichiometric complexes in *h*-BN monolayer can be easily ionized at high charge states, because the more electrons or holes are injected, the more transition levels approach the band edges.

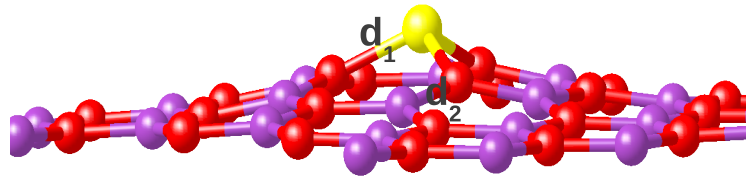


FIG. 4. The optimized local structure of Si_{B1} complex. The distance d_1 is the N-Si bond length and d_2 is the N-B bondlength at the next nearest neighbour with Si impurity.

In the case of neutral charge state, the substitution of Si impurity on the B site (Si_{B1}) causes a significant buckling on the *h*-BN as shown in Fig 4, having the buckling height Δ_h of about 1.10 \AA . The three N atoms surrounding the Si impurity with the equivalent bond lengths d_1 of 1.72 \AA are out of plane. The N-B bond distances d_2 around the Si defect do not show much difference as compared to that of pristine of 1.45 \AA . However, the observed distortion of *h*-BN due to Si impurity is in contrast with the case of the substitution of carbon on the B site C_B , whereby the *h*-BN monolayer becomes flat. The C atom fits well in the *h*-BN monolayer due to its sp^2 bonding

TABLE II. The dependence of the defect-induced structural properties on the various charge states. The Δ_h is the buckling height of Si impurity from the *h*-BN monolayer.

	-2	-1	0	+1	+2
d_1	1.81	1.80	1.72	1.62	1.62
d_2	1.42	1.42	1.44	1.46	1.46
Δ_h	1.28	1.29	1.10	0.41	0.40

nature, similar to *h*-BN monolayer, while the Si impurity is trying to preserve its sp^3 bonding that has relatively large bond lengths.

The addition of a -1 charge into the Si_{B1} complex increases the distance d_1 and buckling height Δ_h of neutral charge state by 0.10 Å and 0.20 Å respectively. This might be due to the coulomb repulsion between the added electron into the Si defect orbital and the valence electrons in the nitrogen orbitals of the same spin. When a hole is added into the Si_{B1} different scenario is noted, the distance d_1 and buckling height Δ_h of neutral charge state decrease by 0.10 Å and 0.69 Å respectively. The addition of the second hole does not impose further significant changes on the structural properties. In the case of carbon substitution, the C-N bond length is 1.41 Å (1.38 Å) when one excess electron (hole) is induced into the system.[35] This reveals that both charges (-1 and +1) significantly reduce the C-N bond length.

Electronic and magnetic properties

To study the electronic and magnetic properties of Si substitutional impurity complexes in *h*-BN monolayer, the electronic densities of states (DOS) were plotted and shown on Fig 6. Fig 5 depicts the DOS of pristine *h*-BN monolayer for comparison purpose. The majority and minority spins are symmetrical for the entire plot, revealing the non-magnetic character in this system. Fig 5 also shows that pristine *h*-BN monolayer is a wide band gap semiconductor.

Fig 6 shows that the Si substitutional impurity complexes introduce new states within the band gap of *h*-BN monolayer. The ground state of most complexes is spin-polarised (majority spin DOS are not equivalent to minority spin DOS) as compared to the pristine *h*-BN monolayer. De-

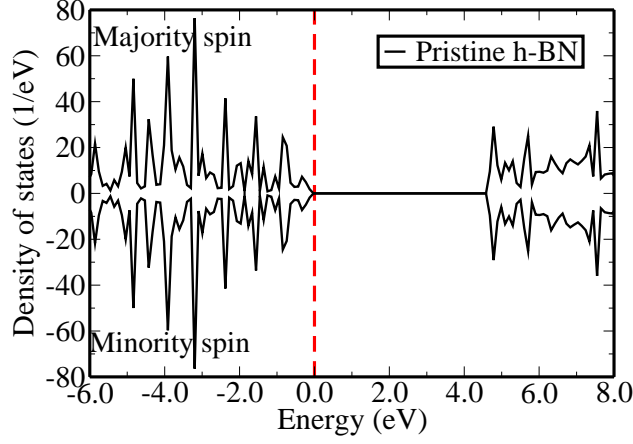


FIG. 5. The spin polarized total density of states of h -BN. The Fermi level (at $E_F = 0$ eV) is shown by the dashed vertical line.

pending on the substitutional site, the induced states appear to be either deep (in the middle of the gap) or shallow (appearing within the gap but close to the band edges). Table III presents the total magnetic moment and magnetization energy ΔE_{mag} of each complex system. The ΔE_{mag} is the energy gained when the spin polarisation is imposed in the calculation and is proportional to Currie temperature. [72] We obtain this energy as the energy difference between the total energy of spin-polarised ground states and that of the non-spin-polarised (non-magnetic) system.

Fig 6(a) depicts the DOS of Si_{B1} complex. Two deep Si impurity spin states in the band gap are noted, in good agreement with Liu *et al.* [47] In the case of C_B , Park et al. [71] reported that the impurity state associated with C is located close to the conduction band. We observe a metallic behaviour in the majority spin channel with the Fermi level lying on the impurity states, while the minority spin component shows a semiconducting behaviour. This confirms that the Si_{B1} complex in h -BN monolayer is half-metallic in nature. The spin ordering of this particular complex is ferromagnetic with a total magnetic moment of $1.00 \mu_B$ and magnetization energy ΔE_{mag} of 0.34 eV. Sato *et al.*[72] reported that in general, if the system is half-metallic, the total magnetic moment should be an integer number. Our findings can be explained using molecular orbital theory as follows: the removal of B atom from h -BN monolayer results in three N dangling bonds. Si impurity on B vacancy site acts as an electron donor due to its lower electronegativity as compared to the N atom. Basically, the Si atom has four valence electrons to donate, however the three N dangling bonds can accept three. The fourth valence electron becomes loosely bound

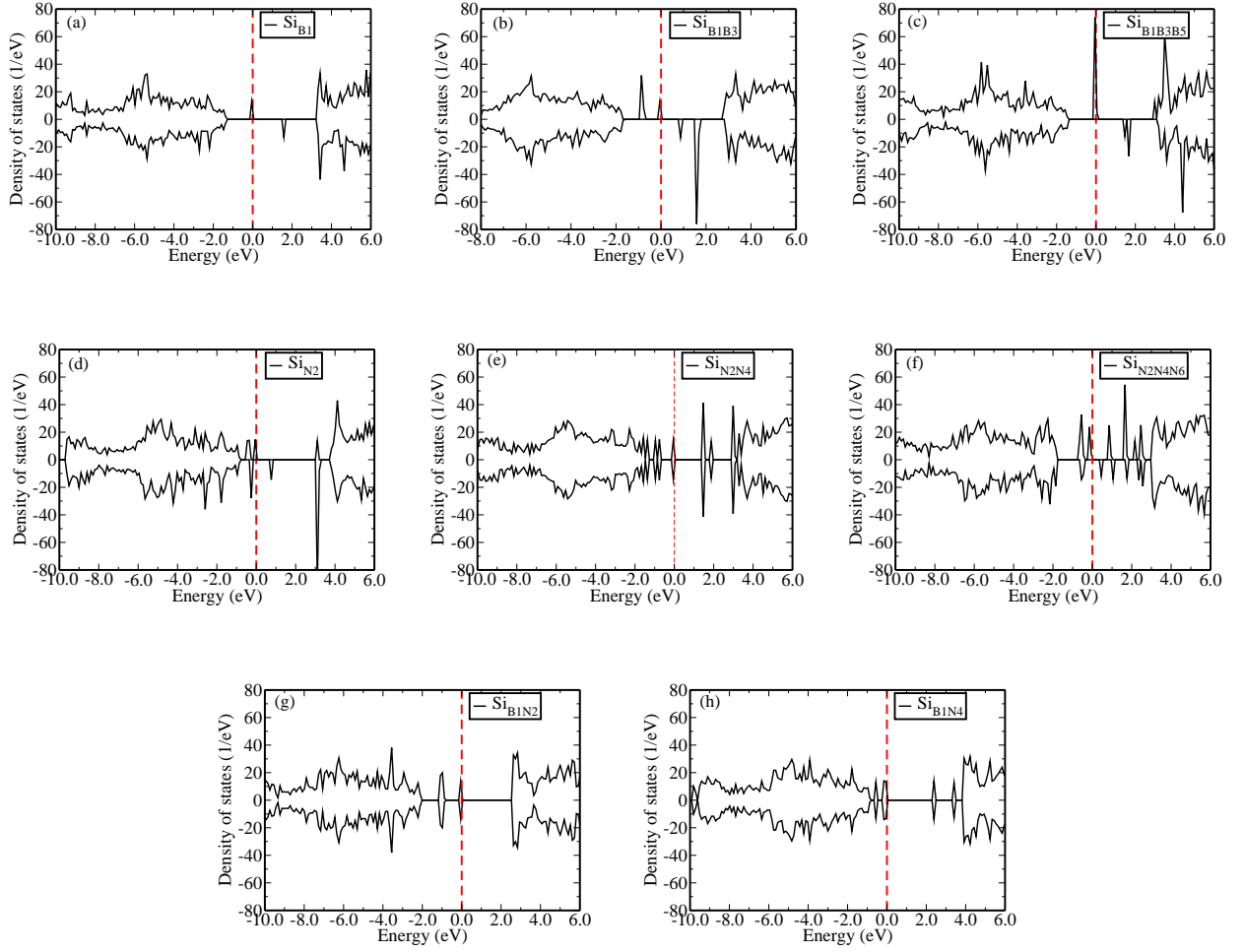


FIG. 6. The spin polarized total density of states of various uncharged Si complexes in *h*-BN. The Fermi level (at $E_F = 0.00$ eV) is shown by the dashed vertical line.

(dangling bond) and lies in a partially occupied p state at the vicinity of the Fermi level. Fig 6(b) depicts the DOS for Si_{B1B3} complex. It is noted that the Si_{B1B3} complex induces more states into the band gap than Si_{B1} . This is not an odd result, because Si_{B1B3} has more loosely bound electrons than the Si_{B1} complex. Nevertheless, the DOS of this complex exhibits half-metallic character. The DOS for the Si_{B1B3B5} complex on Fig 6(c) shows a deep pronounced defect state peak crossing the Fermi level. This implies that majority of localized electrons associated with the three Si impurities incorporated in the B sites in *h*-BN populate around the Fermi level. The Si_{B1B3B5} complex is also half-metallic in nature, and order ferromagnetically with magnetic moment of $3.00 \mu\text{B}$ per cell and magnetization energy of 0.85 eV. We conclude that the creation of a Si cluster will increase the Currie temperature of the *h*-BN sheet.

TABLE III. The calculated magnetization energy $\Delta E_{mag}(eV)$ and total magnetic moment $Tmm(\mu_B)$ of Si complexes in *h*-BN layer. The spin orderings AFM and HMFM stand for antiferromagnetic and half-metallic-ferromagnetic respectively.

Complexes	Spin order	$\Delta E_{mag}(eV)$	$Tmm(\mu_B)$
Si _{B1}	HMFM	0.34	1.00
Si _{N2}	HMFM	0.15	0.91
Si _{B1B3}	HMFM	0.56	2.00
Si _{N2N4}	AFM	0.00	0.00
Si _{B1B3B5}	HMFM	0.85	3.00
Si _{N2N4N6}	HMFM	0.01	1.02
Si _{B1N2}	AFM	0.00	0.00
Si _{B1N4}	AFM	0.00	0.00

To have a significant understanding on the magnetic properties of the energetically favourable complexes (Si_{B1}, Si_{B1B3} and Si_{B1B3B5}), we examine the interaction of partial density of states (PDOS) for Si and *h*-BN monolayer illustrated on Fig. 7. It is evident from Fig. 7 that the half-metallic behaviour revealed in Si_{B1}, Si_{B1B3} and Si_{B1B3B5} complexes mainly originates from *s* and *p* hybridization between 2*p* (B and N), 3*s* (Si) and 3*p* (Si) states. We note that the Si 3*s* and 3*p* partial states make a significant contribution to majority states that cross the Fermi level. Based on this observation it suffices to mention that Si impurity impose half-metallic character in the *h*-BN layer. Based on standard Mulliken population analysis, it was found that each Si atom contributes a magnetic moment of 0.71 μ_B and all three polarized N atoms surrounding Si defect contribute 0.33 μ_B . For the *s* and *p* partial contribution, the 3*s* and 3*p* orbitals contribute 0.26 μ_B and 0.45 μ_B (Si) whereas 2*s* and 2*p* states contribute 0.051 μ_B and 0.28 μ_B (N) respectively.

Figs 6(d, e and f) present the DOS for Si_{N2}, Si_{N2N4} and Si_{N2N4N6} complexes respectively. We note that Si_{N2N4N6} complex manifests more Si impurity states within the band gap of *h*-BN monolayer as compared to other complexes. Even though Si_{N2} and Si_{N2N4N6} complexes have different concentration of Si impurities, order ferromagnetically, possess nearly the same magnetic moment

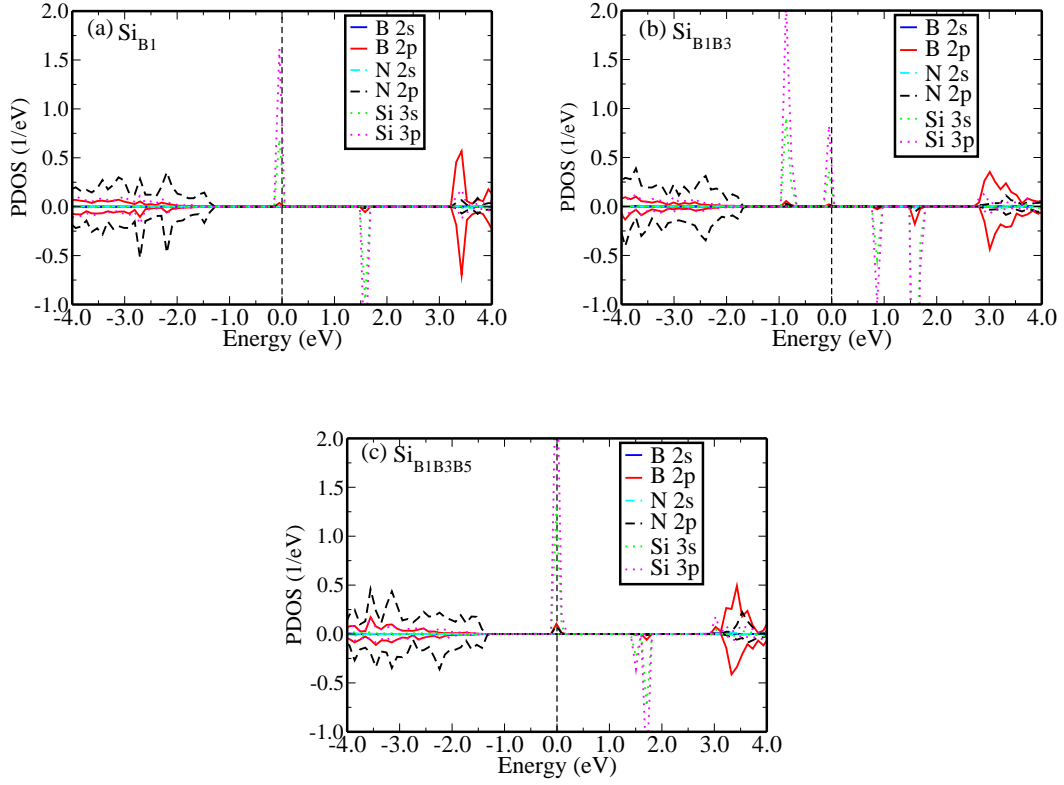


FIG. 7. The spin-polarized partial density of states (PDOS) of Si substitutional complexes (a) Si_{B1} (b) Si_{B1B3} and (c) Si_{B1B3B5} . The Fermi level (at $E_F = 0.00$ eV) is shown by the dashed vertical line.

of almost $1.00 \mu\text{B}$ and have nearly the same magnetization energies (see Table III). The Si_{N2N4} complex orders antiferromagnetically, in the absence of both magnetic moment and magnetization energy. Si impurity in the N site accepts three electrons from its three nearest neighbour B atoms due to high electronegativity and remains with one hole. The observed half-metallic character in the ground state of Si_{N2} and Si_{N2N4N6} might be due to the effect of hole excess, which should be an indication that some orbitals are partially occupied.

The DOS for Si_{B1N2} and Si_{B1N4} are presented on Figs 6(g and h) respectively. It is noted that simultaneous incorporation of Si impurities on both B and N sites result in a non-spin polarized ground state without magnetic moment and magnetization energy. This incorporation is considered to be co-doping, because the composites Si_{B1N2} and Si_{B1N4} involve acceptor (Si_{N2} or Si_{N4}) and donor (Si_{B1}) defects. This compensation enables these complexes to order antiferromagnetically (See Figs 6(g and h)). The DOS for Si_{B1N2} cross the Fermi level deeper than that of Si_{B1N4} complex. The shifting of Fermi level in Si_{B1N2} complex may likely be a result of the formation of

energetically unfavorable sp^3 Si-Si bonding.

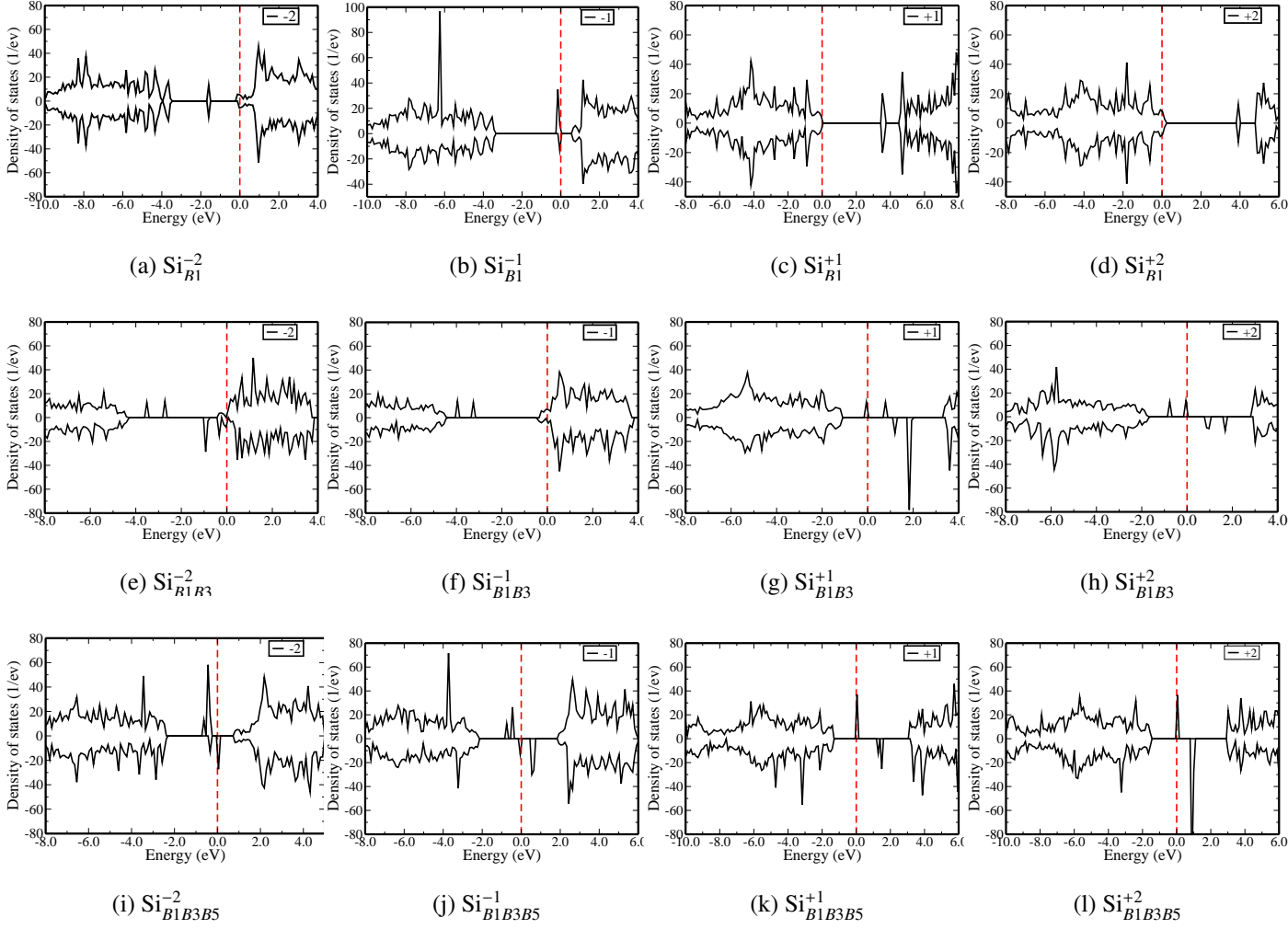


FIG. 8. The spin polarized total density of states for the energetically favourable charged Si complexes in h -BN. The Fermi level (at $E_F = 0$ eV) is shown by the dashed vertical line.

Lastly, we examine the influence of various charge states on the half-metallic character revealed in the Si_{B1} , Si_{B1B3} and Si_{B1B3B5} complexes using the DOS shown on Fig 8. The Fermi levels of systems Si_{B1}^{-1} and Si_{B1}^{-2} appear to be closer to the conduction band edge relative to uncharged (Si_{B1}^0) complex. This implies that these complexes are ready to donate electrons into the conduction band. It is also important to mention that these negatively charged systems (Si_{B1}^{-1} and Si_{B1}^{-2}) possess ferrimagnetic character (at the Fermi level, the magnitude of majority carrier peak is more than the minority carrier peak) with the magnetic moments of $0.65 \mu_B$ and $0.42 \mu_B$ per supercell respectively. On the other hand, the ground state of positively charged complex Si_{B1} (Si_{B1}^{+1} and Si_{B1}^{+2})

is non-spin polarised. These positively charged complexes order antiferromagnetically without magnetic moment. The effect of positive charge state in these complexes shifts the Fermi level towards the valence band revealing the deficiency of electrons in these systems.

Both the negatively charged Si_{B1B3}^{-1} and Si_{B1B3}^{-2} complex systems exhibit ferromagnetic character (shown on Fig 8) with a significant magnetic moment presented on Fig 9. These complex systems manifest donor behaviour by shifting the Fermi level of Si_{B1B3}^0 towards the top of the conduction band edge. The systems Si_{B1B3}^{+1} and Si_{B1B3}^{+2} maintain the half-metallic character of uncharged Si_{B1B3}^0 . The Si_{B1B3}^{+1} yields enhanced magnetic moment of $3 \mu\text{B}$, whereas Si_{B1B3}^{+2} retains the magnetic moment of $2 \mu\text{B}$ as obtained for the neutral Si_{B1B3} . This implies that the induced magnetic moment in these complexes is controllable by an addition or removal of electrons. The charged Si_{B1B3B5}^{-1} , Si_{B1B3B5}^{-2} , Si_{B1B3B5}^{+1} and Si_{B1B3B5}^{+2} systems still retain the induced deep states crossing the Fermi level and order ferromagnetically, albeit with reduced magnetic moments as seen on Fig 9. This implies that a system containing cluster of Si impurities occupying B site in *h*-BN can operate at high electronic or hole charge doping without changing magnetic ordering.

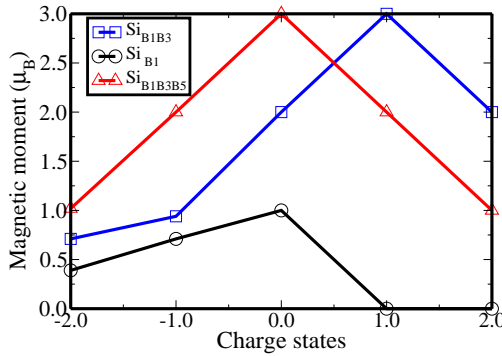


FIG. 9. The dependence of ordered magnetic moments induced by energetically favorable Si substitutional complexes on the charge states $q = -2, -1, 0, +1, +2$.

CONCLUSIONS

Using first-principles DFT methods, we investigated the stability, electronic and magnetic properties of various stoichiometric and non-stoichiometric Si substitutional impurity complexes in

h-BN monolayer. The response of the properties of the most energetically favourable complex to various charge states was also examined. In the case of non-stoichiometric complexes, we found that an enhanced stability is obtained in the environment that corresponds to the high amount of atomic species surrounding Si in the *h*-BN monolayer. The formation of Si in the B site (Si_{B1} , Si_{B1B3} and Si_{B1B3B5}) is exothermic whereas that of Si in the N site (Si_{N2} , Si_{N2N4} and Si_{N2N4N6}) is endothermic, in their respective favourable atmospheric conditions.

The incorporation of Si complexes in the *h*-BN monolayer introduces impurity states into the band gap. Our results indicate that non-stoichiometric complexes tune the non-magnetic ground state in *h*-BN to order half-metallic ferromagnetically. These complexes offer significant magnetic moments and magnetization energies that depend on the number of Si impurities. We revealed that half-metallic character originates from *s* and *p* orbitals hybridization of all atoms involved with a major contribution from the Si impurity 3*s* and 3*p* partial orbital. The formation of stoichiometric Si complexes (Si_{B1N2} and Si_{B1N4}) is independent of growth condition owing to donor-acceptor defects compensation. This compensation leads to these systems to order antiferromagnetically without magnetic moments and magnetization energies.

The properties of non-stoichiometric complexes (Si_{B1} , Si_{B1B3} and Si_{B1B3B5}) have shown great dependence on the charge state and also the position of Fermi level. As μ_e increases, the positively charged Si substitutional complexes show an increase in formation energy from the VBM, while the negatively charged complexes show a decrease towards the CBM. The effect of charge injection also introduces deep thermodynamic transition levels within the band gap. We revealed that magnetism in these complexes is tunable due to charge variation. The Fermi level of positively (negatively) charged Si_{B1} shifts towards CBM (VBM) relative to the uncharged complex, and half-metallic character get lost. The charged cluster Si_{B1B3B5} retains half metallicity and ferromagnetic ordering, despite a decrease in magnetic moment.

ACKNOWLEDGMENTS

The authors would like to thank University of Pretoria and National Research Foundation (NRF) for financial support. NC is also grateful to national institute of theoretical physics (NIThep) for financial support. We are grateful to Prof J. Pretorius and Prof W. Meyer for assistance with VASP code.

* edwin.mapasha@up.ac.za

- [1] K. Watanabe, T. Taniguchi, and H. Kanda, *Nat. Mater.* **3**, 404 (2004).
- [2] D. Pacile, J. C. Meyer, C. O. Girit, and A. Zettl, *Appl. Phys. Lett.* **92**, 133107 (2008).
- [3] N. Alem, R. Erni, C. Kisielowski, M. D. Rossell, W. Gannett, and A. Zettl, *Phys. Rev. B* **80**, 155425 (2009).
- [4] R. V. Gorbachev, I. Riaz, R. R. Nair, R. Jalil, L. Britnell, B. D. Belle, E. W. Hill, K. S. Novoselov, K. Watanabe, T. Taniguchi, A. K. Geim, and P. Blake, *Small*. **7**, 465 (2011).
- [5] J. C. Meyer, A. Chuvilin, G. Algara-Siller, J. Biskupek, and U. Kaiser, *Nano Lett.* **9**, 2683 (2009).
- [6] K. S. Novoselov, A. K. Geim, S. V. Morozov, D. Jiang, Y. Zhang, S. V. Dubonos, I. V. Grigorieva, and A. A. Firsov, *Science* **306**, 666 (2004).
- [7] A. K. Geim and K. S. Novoselov, *Nature Mater.* **6**, 183 (2007).
- [8] P. R. Wallace, *Phys. Rev.* **71**, 622 (1947).
- [9] K. S. Novoselov, A. K. Geim, S. V. Morozov, D. Jiang, Y. Zhang, M. I. Katsnelson, S. V. Dubonos, I. V. Grigorieva, and A. A. Firsov, *Nature (London)* **438**, 197 (2005).
- [10] K. S. Novoselov, Z. Jiang, Y. Zhang, S. V. Morozov, H. L. Stormer, U. Zeitler, J. C. Maan, G. S. Boebinger, P. Kim, and A. K. Geim, *Science* **315**, 1379 (2007).
- [11] L. Song, L. Ci, H. Lu, P. B. Sorokin, C. Jin, J. Ni, A. G. Kvashnin, D. G. Kvashnin, J. Lou, B. I. Yakobson, and P. M. Ajayan, *Nano Lett.* **10**, 3209 (2010)
- [12] D. Golberg, Y. Bando, Y. Huang, T. Terao, M. Mitome, C. Tang, and C. Zhi, *ACS Nano*. **4** 2979-2993 (2010).
- [13] Y. Ma, Y. Dai, M. Guo, C. Niu, L. Yu, and B. Huang, *Nanoscale* **3**, 2301 (2011).
- [14] J. S. Crvenka, M. I. Katsnelson, and C. F. J. Flipse, *Nature Phys.* **5**, 840 (2009).
- [15] R. F. Liu and C. Cheng, *Phys. Rev. B* **76**, 014405 (2007).
- [16] M. S. Si and D. S. Xue *Phys. Rev. B* **75**, 193409 (2007).
- [17] J. M. Pruneda, *Phys. Rev. B* **85**, 045422 (2012).
- [18] X. Wei, M. Wang, Y. Bando, and D. Golberg, *J. Am.Chem. Soc.* **132**, 13592 (2010).
- [19] X. Wei, M. Wang, Y. Bando, and D. Golberg, *ACS Nano* **5**, 29162922 (2011).
- [20] N. Berseneva, A. V. Krasheninnikov, and R. M. Nieminen, *Phys. Rev Lett.* **107**, 035501 (2011).
- [21] A. M. Ukpong and N. Chetty, *Phys. Rev. B* **86**, 195409 (2012).

- [22] R. A. de Groot, F. M. Mueller, P. G. van Engen, and K. H. J. Buschow, *Phys. Rev. Lett.* **50**, 2024 (1983).
- [23] T. Dietl, H. Ohno, F. Matsukura, J. Cibert, and D. Ferrand, *Science* **287**, 1019 (2000).
- [24] T. Dietl, H. Ohno, and F. Matsukura, *Phys. Rev. B* **63**, 195205 (2001).
- [25] S. A. Wolf, D. D. Awschalom, R. A. Buhrman, J. M. Daughton, S. von Molnar, M. L. Roukes, A. Y. Chatcehlkanova, and D. M. Treger, *Science* **294**, 1488 (2001).
- [26] S. Okada, *Phys. Rev. B* **80**, 161404 (2009).
- [27] S. Azevedo, J. R. Kaschny, C. M. C. de Castilho, and F. de BritoMota, *Eur. Phys. J. B* **67**, 507 (2009).
- [28] F. Oba, A. Togo, I. Tanaka, K. Watanabe, and T. Taniguchi, *Phys. Rev. B* **81**, 075125 (2010).
- [29] L.C. Yin, H.-M. Cheng, and R. Saito, *Phys. Rev. B* **81**, 153407 (2010).
- [30] C. Attacalite, M. Bockstedte, A. Marini, A. Rubio, and L. Wirtz, *Phys. Rev. B* **83**, 144115 (2011).
- [31] Y. Kubota, K. Watanabe, O. Tsuda, and T. Taniguchi, *Science* **317**, 932 (2007).
- [32] M. G. Silly, P. Jaffrennou, J. Barjon, J. S. Lauret, F. Ducastelle, A. Loiseau, E. Obraztsova, B. Attal-Tretout, and E. Rosencher, *Phys. Rev. B* **75**, 085205 (2007).
- [33] L. Museur, E. Feldbach, and A. Kanaev, *Phys. Rev. B* **78**, 155204 (2008).
- [34] W. Orellana and H. Chacham, *Phys. Rev. B* **63**, 125205 (2001).
- [35] B. Huang, and H. Lee, *Phys. Rev. B* **86**, 245406 (2012).
- [36] O. L. Krivanek, M. F. Chisholm, V. Nicolosi, T. J. Pennycook, G. J. Corbin, N. Dellby, M. F. Murfitt, C. S. Own, Z. S. Szilagy, M. P. Oxley, S. T. Pantelides, and S. J. Pennycook, *Nature (London)* **464**, 571 (2010).
- [37] Y. Shi, C. Hamsen, X. Jia, K. K. Kim, A. Reina, M. Hofmann, A. L. Hsu, K. Zhang, H. Li, Z.-Y. Juang, M. S. Dresselhaus, L.-J. Li, and J. Kong, *Nano Lett.* **10**, 4134 (2010).
- [38] L. Ci, L. Song, C. Jin, D. Jariwala, D. Wu, Y. Li, A. Srivastava, Z.F. Wang, K. Storr, L. Balicas, F. Liu, P.M. Ajayan, *Nat. Mater.* **9** 430 (2010).
- [39] S.B. Tang, Z.X. Cao, *Phys. Chem. Chem. Phys.* **12** 2313 (2010).
- [40] Y.G. Zhou, J.X. Dong, Z.G. Wang, H.Y. Xiao, F. Gao, X.T. Zu, *Phys. Chem. Chem. Phys.* **12** 7588 (2010).
- [41] Y.G. Zhou, P. Yang, X. Sun, Z.G. Wang, X.T. Zu, F. Gao, *J. Appl. Phys.* **109** 084308 (2011).
- [42] W.Q. Han, W. Mickelson, J. Cumings, *Appl. Phys.* **93**, 1110-1114 (2008).
- [43] B. He, M. Qiu, M. F. Yuen, and W. J. Zhang, *Appl. Phys. Lett.* **05**, 012104 (2014).
- [44] H. Murata, T. Taniguchi, S. Hishita, T. Yamamoto, F. Oba, and I. Tanaka *Journal of applied physics*,

- 114**, 233502 (2013).
- [45] S. Majety, T. C. Doan, J. Li, J. Y. Lin, and H. X. Jiang, *AIP. Advances* **3**, 122116 (2013).
- [46] S. Lin, X. Ye and J. Huang, *Phys. Chem. Chem. Phys.*, **17**,888-95 (2015).
- [47] Y. Liu, B. Gao, D. Xu, H. Wang and J. Zhao, *Phys. Lett. A* **378** 2989-2994 (2014).
- [48] G. Kresse, and J. Hafner *Phys. Rev. B* **47**, 558 (1993).
- [49] G. Kresse, and J. Hafner *Phys. Rev. B* **49**, 14251 (1994).
- [50] G. Kresse, and J. Furthmuller, *Phys. Rev. B* **54**, 11169 (1996).
- [51] G. Kresse, and J. Furthmuller, *Comput. Mater. Sci.* **6**, 11169 (1996).
- [52] J.P. Perdew, K. Burke, M. Ernzerhof, *Phys. Rev. Lett.* **77** 3865 (1996).
- [53] P. E. Blochl, *Phys. Rev. B* **50**, 17953 (1994).
- [54] H. J. Monkhorst and J. D. Pack, *Phys. Rev. B* **13**, 5188 (1976).
- [55] M. Methfessel and A. T. Paxton, *Phys. Rev. B* **40**, 3616 (1989).
- [56] H. Jonsson, G. Mills, and K. W. Jacobsen, in *Classical and Quantum Dynamics in Condensed Phase Simulations*, edited by B. J. Berne, G. Ciccotti, and D. F. Coker (World Scientific, Singapore, 1998), pp. 385.
- [57] G. Mills and H. Jonsson, *Phys. Rev. Lett.* **72**, 1124 (1994).
- [58] G. Henkelman and H. J. Jonsson, *Chem. Phys.* **113**, 9978, (2000).
- [59] H. Yin, I. Pongrac, and P. Ziemann, *J. Appl. Phys* **104**, 023703 (2008)
- [60] T.B. Ngwenya, A.M. Ukpong, and N. Chetty, *Phys. Rev. B* **78**, 245425 (2011).
- [61] S.S. Wise, J.L. Margrave, H.M. Feder, and W.N. Hubbard, *J. Phys. Chem.* **70** 7 (1966).
- [62] C. G. Van de Walle and J. Neugebauer, *J. Appl. Phys.* **95**, 3851 (2004).
- [63] P. Spiewak, K. Sueoka, J. Vanhellefont, K.J. Kurzydowski, K. Mlynarczyk, P. Wabinski, I. Romandic *Phys. B* **401** 205-209 (2007).
- [64] H.-P Komsa, N. Berseneva, A. V. Krasheninnikov, R. M. Nieminen, *Phys. Rev. B* **4**, 031044 (2014).
- [65] J.-Y Noh, H. Kim, and Y.-S. Kim, *Phys. Rev. B* **89**, 205417 (2014).
- [66] D.V. Lang, *J. Appl. Phys.* **45**, 3023 (1974).
- [67] N. Berseneva, A. V. Krasheninnikov, and R. M. Nieminen, *Phys. Rev. Lett.* **107**, 035501 (2011).
- [68] J. Heyd, G. E. Scuseria, and M. Ernzerhof, *J. Chem. Phys.* **118**, 8207 (2003).
- [69] Heyd, G. E. Scuseria, and M. Ernzerhof, *J. Chem. Phys.* **124**, 9906 (2006).
- [70] R. O. Jones, O. Gunnarson, *Rev. Mod. Phys* **61**, 689 (1989).
- [71] H. Park, A. Wadehra, J. W. Wilkins, and A. H. Castro Neto, *Appl. Phys. Lett.*, **100**, 253115 (2012).

- [72] K. Sato, L. Bergqvist, J. Kudrnovsky, P.H.Dederichs, O. Erickson, I. Turek, B. Sanyal, G. Bouzerar, H. Katayama-Yoshima, V.A. Dinh, T. Fukushima, H. Kizaki and R. Zeller, *Rev. Mod. Phys.* **82**, 1633 (2010).